

# Multigrid solution methods for nonlinear time-dependent systems

Feng Wei Yang

Department of Mathematics  
University of Sussex



---

The Leverhulme Trust

---

*F.W.Yang@sussex.ac.uk*

4 December 2014

To solve complex non-linear parabolic systems by applying:

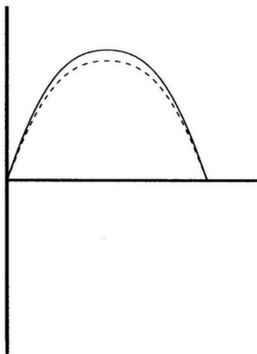
- 2<sup>nd</sup> order central Finite Difference Method (FDM)
- 2<sup>nd</sup> order Backward Differentiation Formula (BDF2)
- Nonlinear multigrid method with Full Approximation Scheme (FAS)
- Adaptive Mesh Refinement (AMR)
- Adaptive time-stepping
- Parallel technique

- Multigrid methods
  - Linear multigrid
  - Nonlinear multigrid
- Thin film models from Gaskell et al.
- Adaptive multigrid solver
- Cahn-Hilliard-Hele-Shaw system of equations from Wise
- Tumour modelling
- Tumour model from Wise et al.
- $2^{nd}$  order convergence rate
- 3-D results

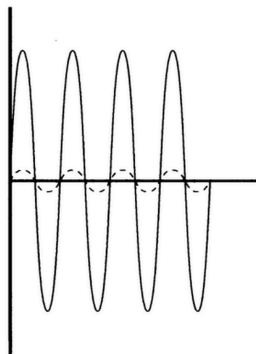
# Jacobi/Gauss-Seidel iterative methods

- Well-known methods
- Require diagonally-dominant matrices
- Typically have complexity of  $\mathcal{O}(n^2)$  for general sparse matrices
- ...
- Smoothing property

Low frequency of error

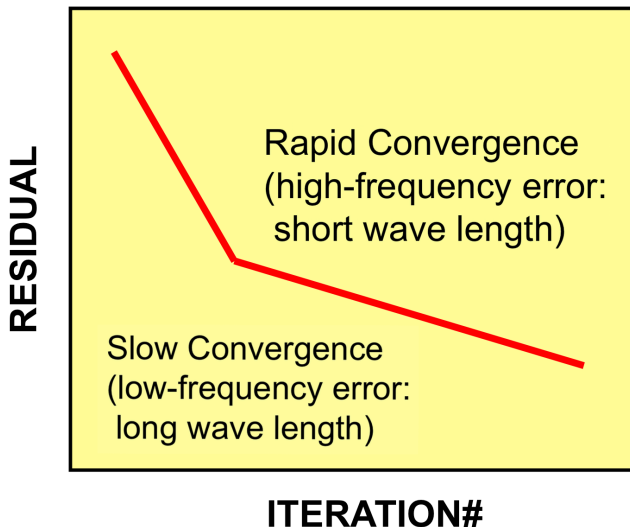


High frequency of error



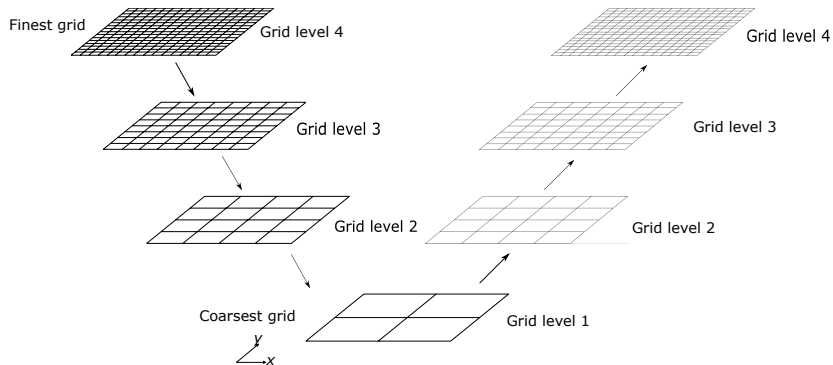
S.H. Lui *Numerical Analysis of Partial Differential Equations*, 2011

# Convergence of a typical Jacobi iterative method



source: [nkl.cc.u-tokyo.ac.jp](http://nkl.cc.u-tokyo.ac.jp)

# Multigrid v-cycle



# Linear multigrid

A linear problem:

$$Au = b, \quad (1)$$

exact error can be obtained as

$$E = u - v, \quad (2)$$

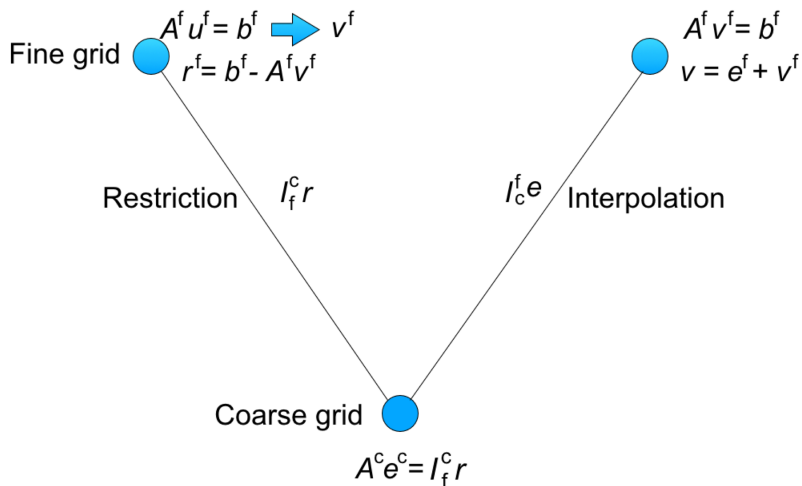
residual can be calculated as:

$$r = b - Av. \quad (3)$$

Error equation:

$$\begin{aligned} AE &= A(u - v) \\ &= Au - Av \\ &= b - Av \\ &= r. \end{aligned} \quad (4)$$

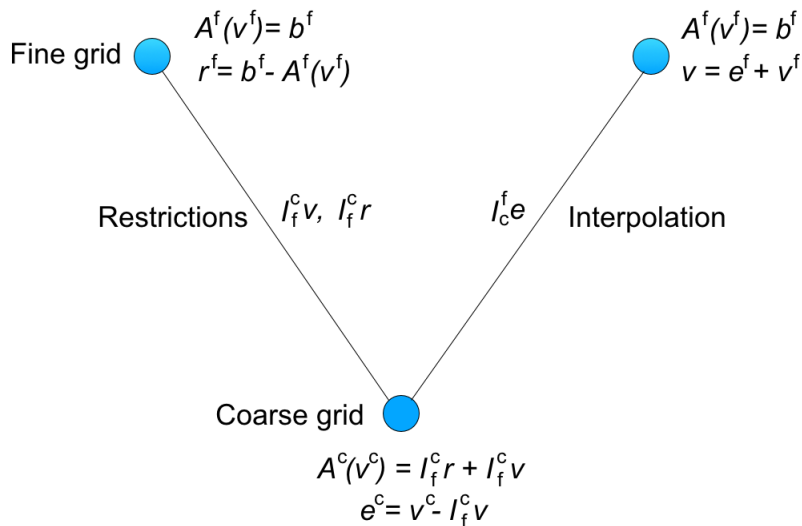
# Linear multigrid





- The Error Equation (4) does not exist in a nonlinear case
- Full Approximate Scheme (FAS)
- For problem on coarser grids, a modified RHS is included

# Nonlinear multigrid

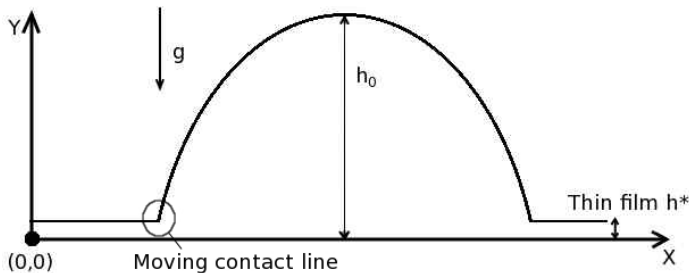


# Droplet spreading model

$$\frac{\partial h}{\partial t} = \frac{\partial}{\partial x} \left[ \frac{h^3}{3} \left( \frac{\partial p}{\partial x} - \frac{B_o}{\epsilon} \sin \alpha \right) \right] + \frac{\partial}{\partial y} \left[ \frac{h^3}{3} \left( \frac{\partial p}{\partial y} \right) \right]$$
$$p = -\Delta(h) - \Pi(h) + B_o h \cos \alpha$$

with Neumann boundary conditions:

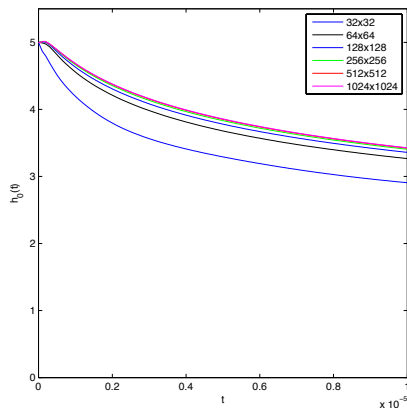
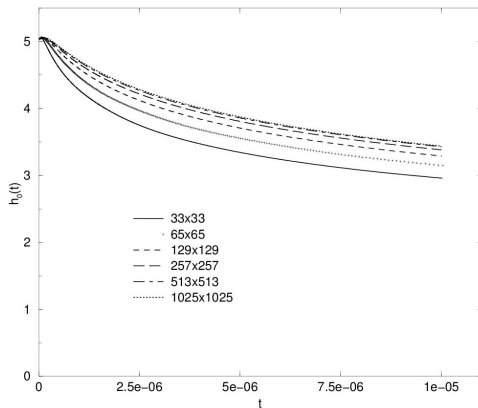
$$\partial_n h = 0 \quad \partial_n p = 0 \quad \text{on } \partial\Omega$$



Gaskell et al. *Int. J. Numer. Meth. Fluids*, 45:1161-1186, 2004

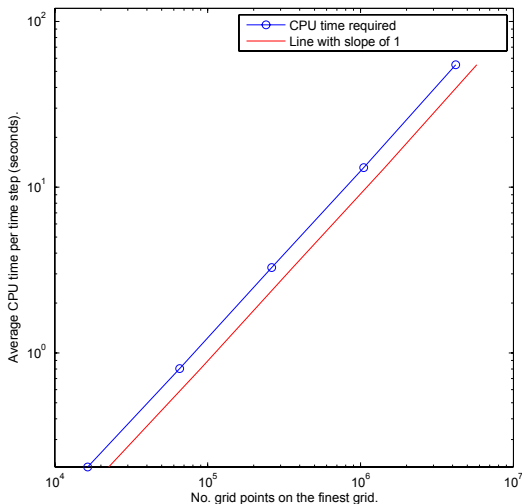
- Cell-centred 2<sup>nd</sup> order finite difference method
- PARAMESH library for mesh generation and AMR
- Fully implicit BDF2 method with adaptive time-stepping
- MLAT variation of FAS multigrid at each time-step
- Newton-block  $2 \times 2$  Red-Black (weighted) Gauss-Seidel smoother
- Full weighting restriction and bilinear interpolation
- Parallelism achieved using ARC2

# Validation



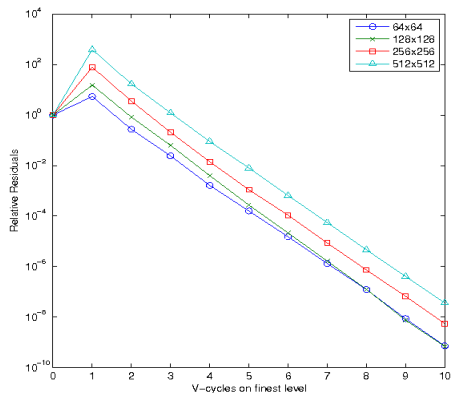
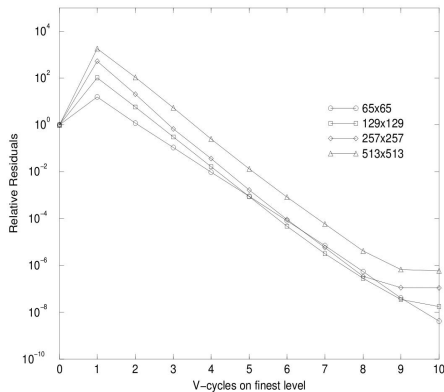
Results from Gaskell et al. on the left and our results on the right.

# Multigrid linear complexity

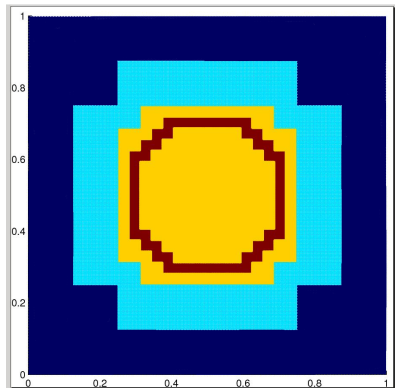
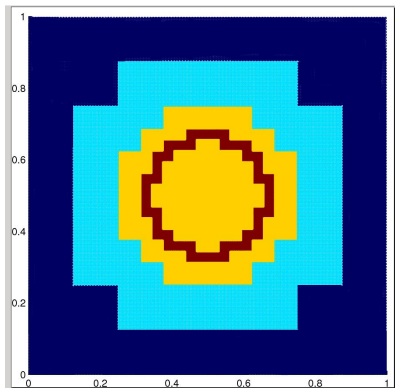


A log-log plot demonstrating the linear complexity of multigrid.

# Multigrid performance



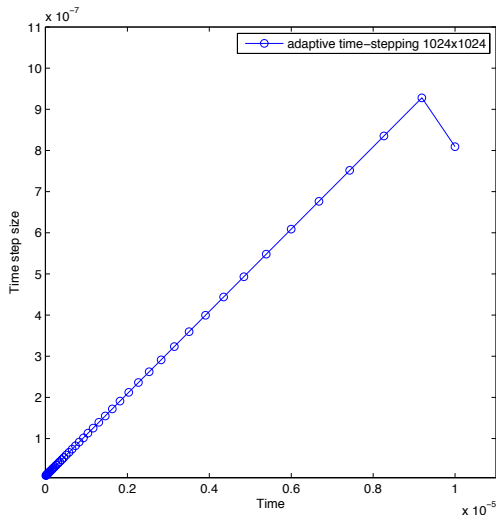
Results from Gaskell et al. on the left and our results on the right.



AMR with initial condition on the left and final solution on the right.

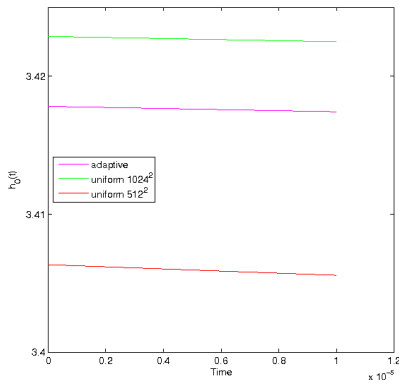


# Adaptive time-stepping



Evolution of  $\delta t$  during  $T = [0, 1 \times 10^{-5}]$ .

# Adaptive multigrid solver



Cases	No. leaf nodes
Uniform 1024 <sup>2</sup>	1,048,576
AMR	168,480

Cases	No. time steps	CPU time (seconds)
Fixed $\delta t$	1000	16721.3
ATS	45	574.4

# Multigrid in parallel

No. cores	1	2	4	8	16	32	64
CPU time (seconds)	3282.6	1687.1	843.5	774.1	490.6	348.6	368.3

**Table:** A grid hierarchy  $16 \times 16 - 1024 \times 1024$ , and mesh block size is  $8 \times 8$ .

No. cores	1	2	4	8	16	32	64
CPU time (seconds)	3264.1	1625.1	840.1	687.3	439.5	351.2	301.7

**Table:** Another grid hierarchy of  $32 \times 32 - 1024 \times 1024$ , and mesh block size of  $8 \times 8$ .

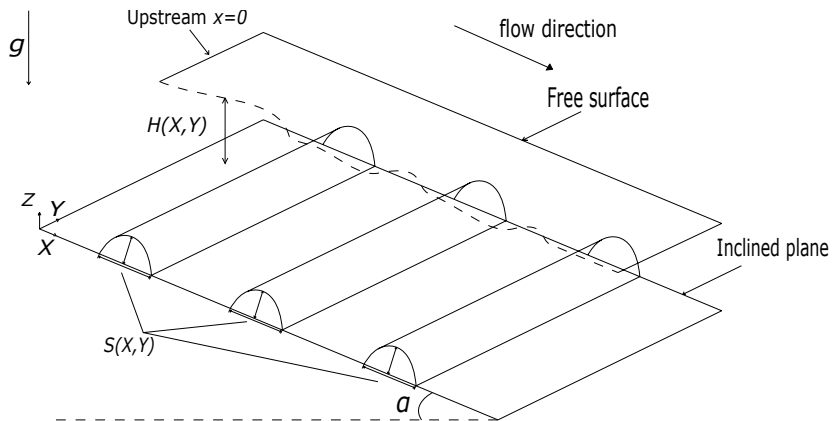
$$\frac{\partial h}{\partial t} = \frac{\partial}{\partial x} \left[ \frac{h^3}{3} \left( \frac{\partial p}{\partial x} - 2 \right) \right] + \frac{\partial}{\partial y} \left[ \frac{h^3}{3} \left( \frac{\partial p}{\partial y} \right) \right]$$
$$p = -6\Delta(h + s) + 2\sqrt[3]{6}N(h + s)$$

with mixed boundary conditions:

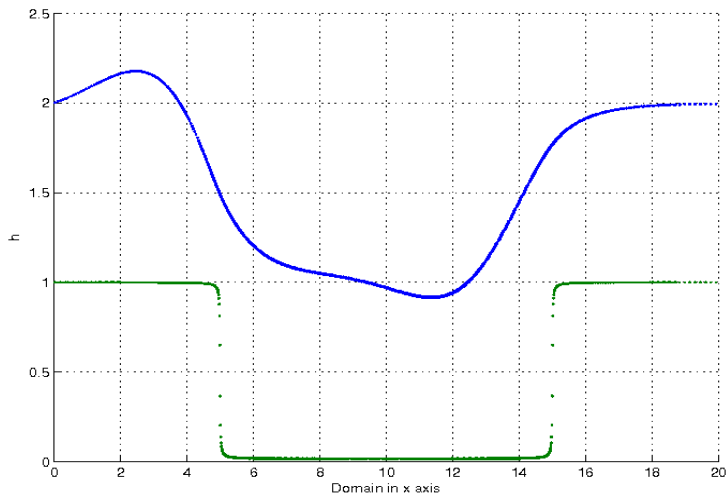
$$h(x=0, y) = g, \quad \frac{\partial p}{\partial x}|_{x=0} = 0, \quad \frac{\partial h}{\partial x}|_{x=1} = \frac{\partial p}{\partial x}|_{x=1} = 0,$$
$$\frac{\partial p}{\partial y}|_{y=0} = \frac{\partial p}{\partial y}|_{y=1} = \frac{\partial h}{\partial y}|_{y=0} = \frac{\partial h}{\partial y}|_{y=1} = 0.$$

Gaskell et al. *J. Fluids Mech.*, 509:253-280, 2004

# Sketch of the fully-developed flow



# Our results with a trench topography



# Cahn-Hilliard-Hele-Shaw system of equations

$$\begin{aligned}\frac{\partial \phi}{\partial t} &= \Delta \mu - \nabla \cdot (\phi \mathbf{u}), \\ \mu &= \phi^3 - \phi - \epsilon^2 \Delta \phi, \\ \mathbf{u} &= -\nabla p - \gamma \phi \nabla \mu, \\ \nabla \cdot \mathbf{u} &= 0,\end{aligned}$$

with Neumann boundary conditions:

$$\partial_n \phi = \partial_n \mu = \partial_n p = 0 \quad \text{on} \quad \partial \Omega,$$

*Wise J. Sci. Comput.*, 44:38-68, 2010

# Cahn-Hilliard-Hele-Shaw system of equations

$$\begin{aligned}\frac{\partial \phi}{\partial t} &= \nabla \cdot (M(\phi) \nabla \mu) - \nabla \cdot (\phi \nabla p), \\ \mu &= \phi^3 - \phi - \epsilon^2 \Delta \phi, \\ -\Delta p &= \gamma \nabla \cdot (\phi \nabla \mu),\end{aligned}$$

with Neumann boundary conditions:

$$\partial_n \phi = \partial_n \mu = \partial_n p = 0 \quad \text{on} \quad \partial \Omega,$$

*Wise J. Sci. Comput.*, 44:38-68, 2010



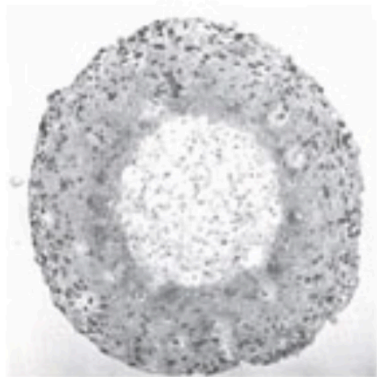
## $2^{nd}$ order convergence rate

For variable $\phi$					
Levels	Time steps	Infinity norm	Ratio	Two norm	Ratio
3	40	-	-	-	-
4	80	$1.074 \times 10^{-3}$	-	$3.885 \times 10^{-4}$	-
5	160	$2.718 \times 10^{-4}$	3.95	$9.781 \times 10^{-5}$	3.97
6	320	$6.905 \times 10^{-5}$	3.93	$2.468 \times 10^{-5}$	3.96

Table:  $2^{nd}$  order convergence rate seen from CHHS system of equations.

# Tumour modelling - avascular tumour growth

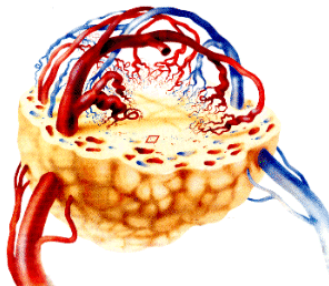
- Starts with a small cluster of cells
- Nutrient supply through diffusion
- Internal adhesion force
- Three layers of cells:
  - Proliferative cells
  - Dormant cells
  - Dead cells (necrosis)
- Volume loss in necrotic core



source: [www.bioinfo.de](http://www.bioinfo.de)

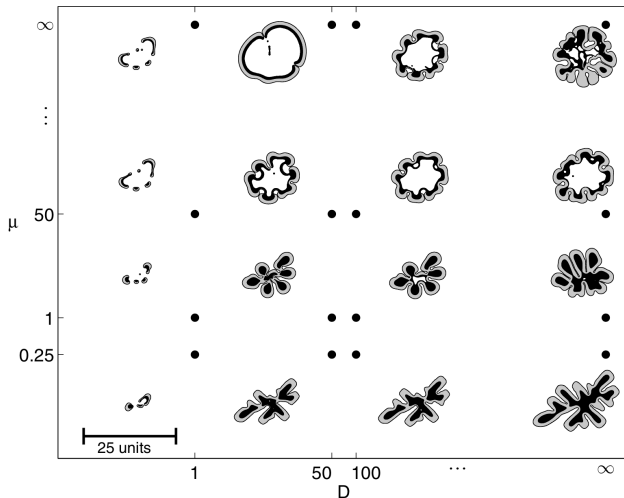
# Tumour modelling - vascular tumour growth

- TAF chemical factor
- Inducing blood vessel (angiogenesis)
- Exponential growth rate
- Develop secondaries through metastasis



source: [www.maths.dundee.ac.uk](http://www.maths.dundee.ac.uk)

# Tumour modelling - micro-environments



J. S. Lowengrub, H. B. Frieboes, Y-L. Chuang, F. Jin, X. Li P. Macklin, S. M. Wise,

*Nonlinearity* 23:R1-R91, 2010

# Tumour model from Wise et al.

$$\begin{aligned}\partial_t \phi_T &= M \nabla \cdot (\phi_T \nabla \mu) + S_T(\phi_T, \phi_D, n) - \nabla \cdot (\mathbf{u}_S \phi_T) \\ \mu &= f'(\phi_T) - \epsilon^2 \Delta \phi_T \\ \partial_t \phi_D &= M \nabla \cdot (\phi_D \nabla \mu) + S_D(\phi_T, \phi_D, n) - \nabla \cdot (\mathbf{u}_S \phi_D) \\ \mathbf{u}_S &= -(\nabla p - \frac{\gamma}{\epsilon} \mu \nabla \phi_T) \\ \nabla \cdot \mathbf{u}_S &= S_T(\phi_T, \phi_D, n) \\ 0 &= \Delta n + T_C(\phi_T, n) - n(\phi_T - \phi_D)\end{aligned}$$

with mixed boundary conditions:

$$\mu = p = 0 \quad n = 1 \quad \partial_n \phi_T = \partial_n \phi_D = 0 \quad \text{on } \partial\Omega,$$

S. M. Wise, J. S. Lowengrub, V. Cristini,

*Math. Comput. Modelling*, 53: 1-20, 2011.

# Tumour model from Wise et al.

$$\begin{aligned}\partial_t \phi_T &= M \nabla \cdot (\phi_T \nabla \mu) + S_T(\phi_T, \phi_D, n) - \nabla \cdot (\mathbf{u}_S \phi_T) \\ \mu &= f'(\phi_T) - \epsilon^2 \Delta \phi_T \\ \partial_t \phi_D &= M \nabla \cdot (\phi_D \nabla \mu) + S_D(\phi_T, \phi_D, n) - \nabla \cdot (\mathbf{u}_S \phi_D) \\ [\mathbf{u}_S &= -(\nabla p - \frac{\gamma}{\epsilon} \mu \nabla \phi_T)] \\ -\Delta p &= S_T(\phi_T, \phi_D, n) - \nabla \cdot (\frac{\gamma}{\epsilon} \mu \nabla \phi_T) \\ 0 &= \Delta n + T_C(\phi_T, n) - n(\phi_T - \phi_D)\end{aligned}$$

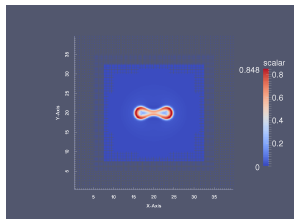
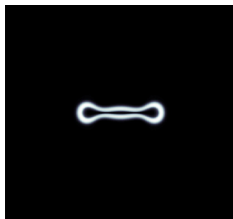
with mixed boundary conditions:

$$\mu = p = 0 \quad n = 1 \quad \partial_n \phi_T = \partial_n \phi_D = 0 \quad \text{on } \partial\Omega,$$

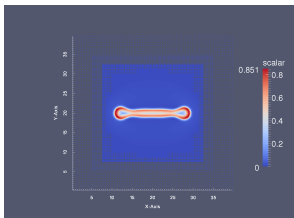
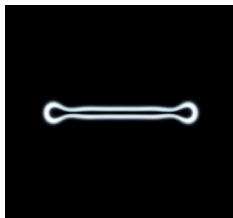
S. M. Wise, J. S. Lowengrub, V. Cristini,

*Math. Comput. Modelling*, 53: 1-20, 2011.

$t=100$



$t=200$



Validation between results of Wise et al. and ours.

## $2^{nd}$ order convergence rate

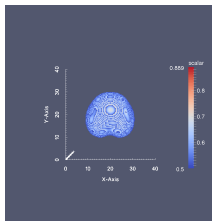
For variable $\phi_T$					
Levels	Time steps	Infinity norm	Ratio	Two norm	Ratio
5( $128^2$ )	1250	-	-	-	-
6( $256^2$ )	2500	$9.118 \times 10^{-2}$	-	$7.836 \times 10^{-3}$	-
7( $512^2$ )	5000	$1.322 \times 10^{-2}$	6.90	$1.131 \times 10^{-3}$	6.93
8( $1024^2$ )	10000	$2.579 \times 10^{-3}$	5.13	$2.367 \times 10^{-4}$	4.78
9( $2048^2$ )	20000	$6.415 \times 10^{-4}$	4.02	$5.833 \times 10^{-5}$	4.06

$2^{nd}$  order convergence rate seen from the model of tumour growth.

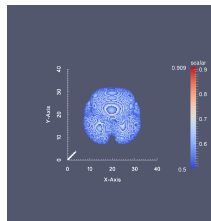


# 3-D results

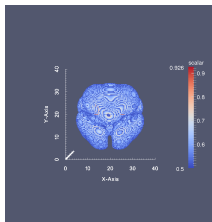
$t=50$



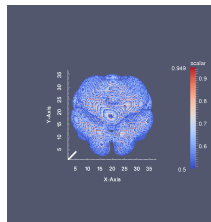
$t=100$



$t=150$

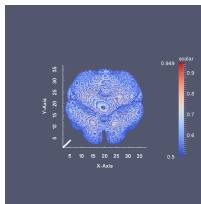


$t=200$

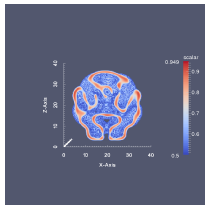


# 3-D results

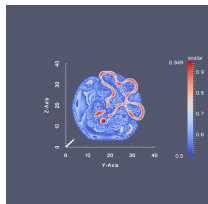
$t=200$



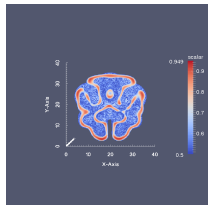
*Cutting through  
y plane*



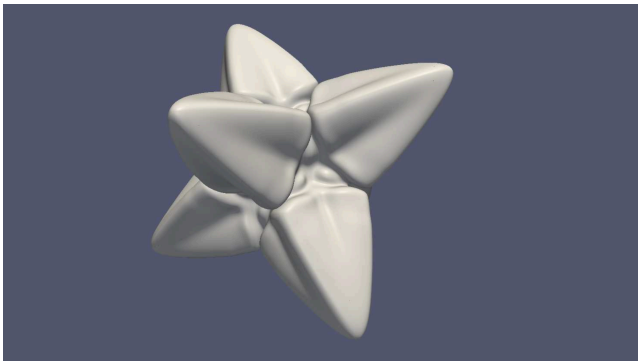
*Cutting through  
x plane*



*Cutting through  
z plane*



# The End



P. C. Bollada, C. E. Goodyer, P. K. Jimack, A. M. Mullis, F. Yang

*J. Comput. Phys.*, submitted 2014